
Article:
Suslovaite, V. orcid.org/0000-0002-3982-4977, Pickett, H., Speight, V. orcid.org/0000-0001-7780-7863 et al. (1 more author) (2024) Forecasting acute rainfall driven E. coli impacts in inland rivers based on sewer monitoring and field runoff. Water Research, 248. 120838. ISSN: 0043-1354

https://doi.org/10.1016/j.watres.2023.120838

Water Research 248 (2024) 120838

Contents lists available at ScienceDirect

Water Research

journal homepage: www.elsevier.com/locate/watres

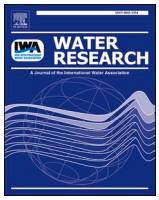

Forecasting acute rainfall driven *E. coli* impacts in inland rivers based on sewer monitoring and field runoff

Vaida Suslovaite [a,*], Helen Pickett [b], Vanessa Speight [a], James D. Shucksmith [a]

[a] Sheffield Water Centre, Department of Civil and Structural Engineering, University of Sheffield, Sheffield S1 3JD, UK
[b] Severn Trent Centre, 2 St Johns Street, Coventry CV1 2LZ, UK

ARTICLE INFO

Keywords:
E. coli modelling
Sewer overflows
Diffuse pollution
Surface water quality
River impact

ABSTRACT

Surface water quality is frequently impacted by acute rainfall driven pollutant sources such as sewer overflows. Understanding the risk of exposure from faecal pollution from short term impacts is challenging due to a paucity of high-resolution data from river systems. This paper proposes practical modelling approach for forecasting arrival time and durations of elevated *E. coli* levels based on hydrological routing of catchment source loadings, characterized by distributed and remote sensing techniques (including sewer overflow monitoring). The model is calibrated and validated using new high resolution *E. coli* datasets from a UK catchment featuring both diffuse field runoff and storm overflow impacts. Hourly/Bihourly sampling of *E. coli* was undertaken in the river following different rainfall events across a range of seasonal conditions. The model provides a good estimate of arrival times and durations of elevated *E. coli* periods following rainfall events. Model simulations suggest that key sources in the catchment are event specific, with sewer overflow spills being more significant following short, intense rainfall events.

1. Introduction

Developing understanding of the fate, transport and survival of faecally derived microorganisms in river systems is a requirement for improving the effective and safe management of water resources (DWI, 2020; Dienus et al., 2016; Graydon et al., 2022), and for health risk assessments associated with recreational activities undertaken in water bodies (Bathing Water Regulations 2013; Marsalek and Rochfort, 2004; Boehm and Soller, 2020). In many countries, the quality of surface water bodies has come under increasing recent focus due to increased spill frequency monitoring of storm sewer overflows (SSOs) and public demand for designated bathing water sites (Zan et al., 2023). For example, in the UK the Environment Act (2021) has recently increased requirements for the direct monitoring of water quality impacts of SSOs. Whilst the robust direct real time measurement of microbial water quality remains unproven (Demeter et al., 2020; Burnet et al., 2021), modelling tools can potentially consider and provide warning of periods of elevated risk to surface water sources and public health. However, the development of widely applicable, generalized tools to understand faecal pollution and associated risks in surface waters remains challenging, especially those caused by acute impacts with high temporal variability (Taghipour et al., 2019; Kammouna at al., 2023). A number of studies have conducted detailed monitoring and/or small scale modelling to understand spatial and temporal dynamics of *E. coli* at individual river reaches, or in small agricultural sub catchments (e.g. Hellweger and Masopust, 2008; Sokolova et al., 2013; Gao et al., 2015; Neill et al., 2020). However, there is a current lack of well validated modelling methodologies for acute impacts that can be applied in mixed use (i.e. urban and rural) catchments, without extensive characterisation of sources and the use of detailed 2D/3D hydrodynamic modelling (and associated topographic surveys). Further, forecasting models for early warning applications (such as water abstraction management or bathing water alerts) require input datasets which characterise source loadings that can be collected and communicated remotely and be available in near real time (Seis et al., 2018; Yassin et al., 2021).

Many studies utilize *E. coli* counts as an indicator of faecal contamination in waterbodies (Madoux-Humery et al., 2013). However, the conventional microbial analysis of water quality samples is relatively time/resource intensive. For example, the membrane filtration method (standard used by the UK water industry), involves dilution (if needed), filtration and incubation of the sample for a minimum of 18 h (The Standing Committee of Analysts, 2016). The characterization of the

* Corresponding author.
E-mail address: vsuslovaite1@sheffield.ac.uk (V. Suslovaite).

https://doi.org/10.1016/j.watres.2023.120838
Received 22 August 2023; Received in revised form 29 October 2023; Accepted 3 November 2023
Available online 4 November 2023

microbial quality of surface waters is therefore commonly based on sampling and analysis conducted at relativity coarse resolution in relation to the temporal dynamics of potential rainfall driven sources, and hence can neglect the full influence of SSOs which may only discharge for a few hours (Seis et al., 2018; Madoux-Humery et al., 2016; Jalliffier-Verne et al., 2017; Shepherd et al., 2023). Further, a number of previous studies have shown that a significant source of faecal contamination in rivers within mixed catchments is diffuse, rainfall-driven runoff, with risks particularly high during elevated flow events due to contaminated runoff from pastoral farmland which also commonly exhibits high temporal variability at sub hourly timescales (Oliver et al., 2009; Ghimire and Deng, 2013; McKergow and Davies--Colley, 2010; Jovanovic et al., 2017; Buckerfield et al., 2019; Hubbart et al., 2022). The mismatch in monitoring practice and timescales of key water quality processes mean that significance of many accumulation and transport processes is currently poorly understood, particularly those which may dominate acute impacts over shorter timescales, such as mixing and dispersion processes in river and streams (Camacho Suarez et al., 2019a), spatially variable rainfall runoff and associated processes (Jovanovic et al., 2017) and volumes and loadings from individual highly intermittent SSOs (Madoux-Humery et al., 2015; Owolabi et al., 2022). Many existing approaches widely applied to predict diffuse pollution exposure in surface water bodies are developed with a view to analysing long-term effects of catchment management practices and are often calibrated and validated with relatively coarse datasets (daily and above). (Sadeghi and Arnold, 2002; Collins and Rutherford, 2004; Dorner et al., 2006; Ferguson et al., 2007; Walker and Stedinger, 1999; Whelan et al., 2014; Haydon and Deletic, 2006; Schijven et al., al.2015; Sterk et al., 2016; Brannan et al., 2002). As a result, many existing catchment scale water quality models lack detailed representation of spatio-temporally distributed surface runoff generation from source areas, intermittent point loadings (e.g. from SSOs) and transport processes and hydrological pathways throughout the catchment. However this is likely to be required for accurate prediction of the arrival of temporally variable short-term (sub daily) peak concentrations of pollutants following rainfall events (Asfaw et al., 2018; Buckerfield et al., 2019). This limits such process based models applicability and viability for forecasting applications such as active water abstraction management (Yassin et al., 2021) or real time bathing water condition modelling/early warning (Seis et al., 2018). There is therefore a need to develop and validate new, practically applicable forecasting tools for feacal contamination that can be applied at catchment scales and consider acute inputs from both agricultural and urban sources. In addition to a lack of water quality data at appropriate resolution for calibration and validation, further challenges associated with the modelling of faecal contamination include high inherent parametric and structural uncertainties associated with modelling loadings from inputs such as SSOs and diffuse agricultural runoff (Srivastava et al., 2018; Tscheikner-Gratl et al., 2019).

The lack of integrated monitoring and modelling capabilities of acute impacts across the urban drainage and catchment domains, means that quantifying the relative scale and nature of risks to water resource systems from different potential sources (e.g. SSOs vs rural diffuse runoff) is also practically difficult (Derx et al., 2023). The recent use of microbial source tracking techniques has been shown to successfully elucidate potential sources (Joseph et al., 2021; Wiesner-Fridman et al. 2022; Zan et al., 2023). However, the present cost and complexity of such techniques means that they are generally only applied to a limited number of samples, which may not provide a representative apportionment of source loadings over longer timescales.

Despite challenges, in recent years the quality and quantity of spatially distributed environmental datasets of concern to water applications has increased, including radar rainfall data, remote sensing of soil condition and land use, and in some cases such as in the U.K., datasets concerning timing of SSO discharges from urban drainage networks. Further to this, the use of automated sampling techniques has simplified the logistics concerning the collection of high resolution water quality samples. The potential for real time sensing/monitoring of feacal pollution is also a subject of current research, for example based on fluorescence-based detection of the enzymatic activity (Demeter et al., 2020; Burnet et al., 2021), however the reported performance of such techniques for *E. coli* measurement is variable across different waterbody types. Whilst these tools provide potential to improve understanding of short-term dynamics in surface runoff-based generation and transport, many of approaches/datasets have yet to be integrated into river impact models or fully deployed to characterise and assess the significance of acute loadings of Faecal Indicator Organisms (FIOs) into receiving waters. For example, to the authors knowledge the use of directly monitored SSO water levels as an alternative to hydrodynamic and water quality modelling of an urban drainage network to estimate SSO impacts has not been previously attempted.

The aim of this work is to develop a novel, practically applicable process-based forecasting approach to characterize short term *E. coli* dynamics in catchment scale river networks, considering both inputs from SSO discharges and diffuse agricultural runoff. The model application is focused on providing advanced warning of water quality issues at a water abstraction site, although a similar model structure may be considered for forecasting the quality of recreational waters. As such, understanding the arrival time and duration of elevated loadings within the river network following commonly occurring rainfall events is the primary objective of the model. The approach is based on the temporal routing of individual source areas (based on land use) within the catchment through the river network, considering spatially variable rainfall runoff processes (for agricultural areas), and the novel use of hydraulic monitoring data from individual SSO sites provided by the water infrastructure operator. The model is calibrated and validated against new hourly/bihourly datasets of *E. coli* concentrations in a UK case study catchment featuring both agricultural and SSO inputs, collected during and after rainfall events over a range of seasonal conditions. The model outputs are further used to consider the relative significance of urban and rural sources in the catchment area over diffrent seasons.

2. Methodology

This section describes the case study catchment area, sampling and microbial water quality analysis procedure as well as the development of a modelling approach to describe short-term fluxes of *E. coli* in response to individual rainfall runoff and SSO discharge events.

2.1. Study area

The River Leam is a 300km^2 sub catchment of River Severn with elevation ranging from 46 m to 232 m above sea level. A surface water abstraction site is maintained by the utility operator for potable water supply (Fig. 1), situated at the catchment outlet. Agriculture is the dominant catchment land use with predominantly clayey and loamy soils. Several urban, suburban and rural developments are also present in the catchment, totalling 12.83 km^2 of built-up area (Ordnance Survey, 2023), with predominantly combined urban drainage systems also maintained by the utility operator alongside a number of associated SSO outfalls. A UK Environment Agency (EA) flow gauging station is situated at the outlet of the catchment to monitor abstraction license restrictions. The normal flow depth of the River Leam at the gauging station ranges between 0.24 m and 1.16 m with an average flow of 1.55 m^3/s (Q70; 0.319 m^3/s, Q50; 0.441 m^3/s, Q10; 3.573 m^3/s) and mean annual catchment rainfall of 649 mm (NRFA, 2023). The catchment has previously been used to develop a rainfall runoff model to forecast the arrival of pesticides at the abstraction point caused by field runoff (Asfaw et al., 2018). Based on long term routine monitoring at the abstraction site, the utility operator has identified faecal pollution after rainfall events as a further water quality concern.

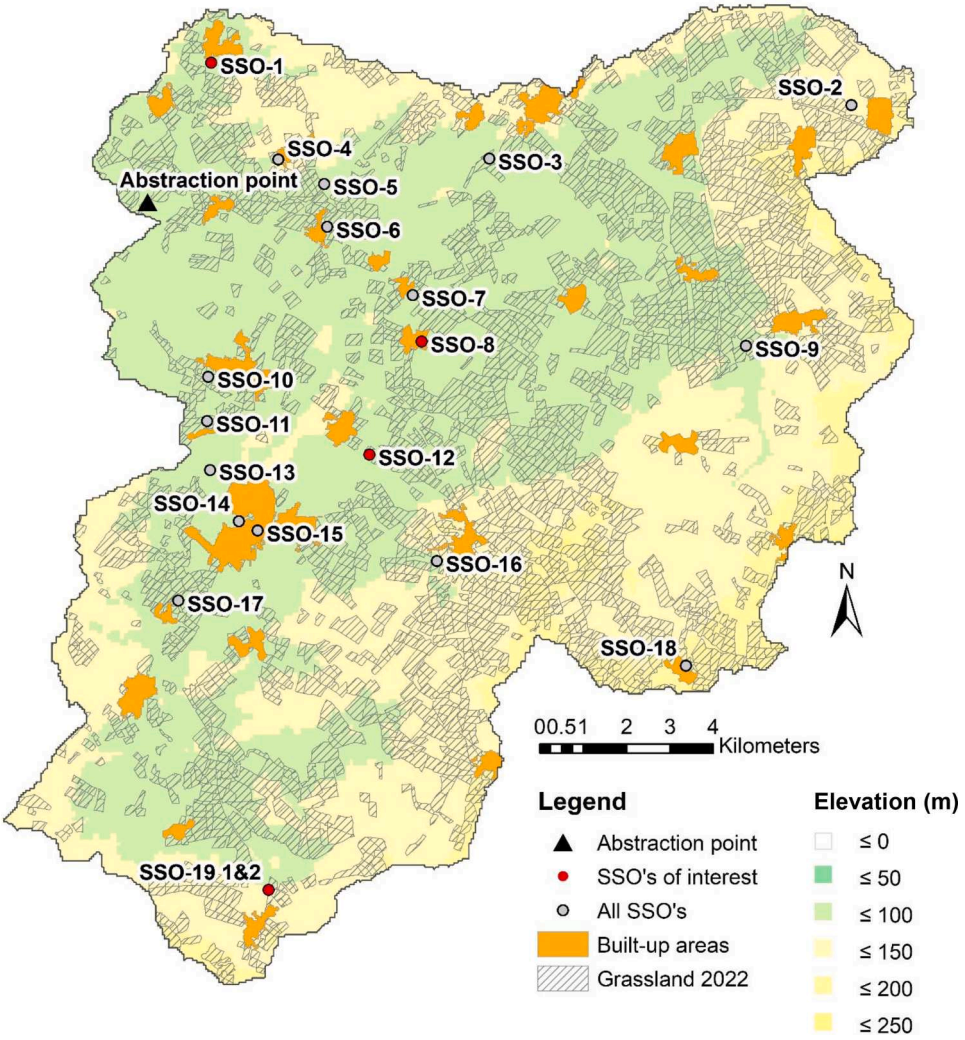

Fig. 1. Study catchment map showing elevation (meters above sea level) the locations of SSO's, built up areas and grassland for livestock grazing.

2.2. Development of E. coli modelling approach

Based on the available catchment information, the major sources of acute rainfall driven FIOs in the catchment are assumed to be field runoff from pastoral agricultural land, and SSO spills. The proposed model therefore accounts for SSO loadings and agricultural runoff sources for given rainfall events as identified by catchment land use and asset data. During rainfall events travel times from sources to a monitoring point at the catchment outlet are based on a travel time approach utilizing an existing surface runoff model of the catchment presented in Asfaw et al. (2018). Surface runoff is calculated based on overland flow generated from 5 m^2 grid cells in the catchment utilizing radar rainfall data. The travel time based surface runoff routing method estimates storm runoff transport from catchment grid cells to the outlet of the catchment based on a Geographic Information System (GIS) method. The spatially distributed time variant direct runoff travel time technique employed in the model accounts for spatial and temporal variability of runoff generation and flow routing through overland flows and stream networks (Melesse and Graham, 2004; Du et al., 2009) following rainfall events at a 1 h resolution.

Diffuse *E. coli* loadings are estimated based on build-up functions associated with grazing animals in high risk areas (grasslands) and its wash-off to water courses during surface runoff processes (Oliver et al., 2009). SSO impacts are based on level data from Storm Overflow monitors collected at 15 min resolution and used to estimate volumes and loadings entering the surface waters at each timestep from SSO sites. Loadings from significant SSOs and grassland areas are then routed to the catchment outlet. Diffuse and SSO impacts are integrated and combined model to enable rainfall event based prediction of *E. coli* concentrations at the catchment outlet after rainfall events.

The underlying surface runoff, diffuse pollution and SSO modelling approaches are described in further detail in the following sections.

2.3. Surface runoff modelling

A hydrological model based on the differential form of the Soil Conservation Service curve number method (Mancini and Rosso (1989) has been previously developed and tested within the same catchment (Asfaw et al., 2018), and hence is not reproduced here in detail. Runoff routing is performed using a time varying travel time computation technique, based on flow pathways defined via a GIS flow direction tool based on the catchment digital elevation model. Output surface flow hydrographs at the catchment outlet are based on cumulative excess rainfall travel times from each grid cell, based on kinematic wave theory Wong (2003). Further details of the model setup and initial validation can be found in Asfaw et al. (2018). To ensure robustness of the approach for this study, the model was evaluated during three further wet weather events, during which the model was compared against monitored EA gauging station data (see Section 4.1.). Based on this testing, model antecedent moisture conditions were modified to be

evaluated based on the preceding 25 days of cumulative rainfall data.

2.4. Diffuse faecal pollution loading and routing

The diffuse modelling component estimates the build-up of *E. coli* loading on grazing land within the catchment, and subsequent wash-off during surface runoff events following each rainfall event . Grassland/grazing areas were derived from satellite imagery, acquired from the Centre of Ecology and Hydrology (CEH, 2023) for the period covered in this work (2021–2023). The methodology is based on the approach of Oliver et al. (2009), who developed a method to estimate *E. coli* loadings on fields based on 'a worst case scenario' which represented a realistic upper level of stocking densities in the UK. The concentration of *E. coli* (CFU/m^2) on grassland for a given Julian day (E_x) is calculated as the sum of the daily fresh input of *E. coli* (Ein_x) by grazing livestock and the previous *E. coli* burden, which estimated as a declining due of first-order die-off relationship (see Table 1):

$$E_x = Ein_x + E_{x-1} * e^{-b} \quad (1)$$

Where Ein_x (Colony Forming Units, CFU) are fresh E coli deposits, E_{x-1} (CFU) is the *E. coli* store from the previous day, and *b* is the appropriate seasonal exponential die-off constant. The ovine and bovine die-off constants (Table 1) are higher for the summer (Avery et al., 2004) and lower for the winter months (Oliver et al., 2009).

E. coli deposits are estimated using livestock numbers supplied by DEFRA at UK county level (DEFRA, 2022), multiplied by daily load of *E. coli* excreted by each livestock type during the assumed grazing period (based on the method of Oliver et al., 2009). The number and type of animals is assumed to be equally distributed over the entire grassland area of the catchment. The daily *E. coli* burden in each 5m^2 cell is summed up for each livestock type present and used to calculate daily fresh deposit totals during grazing periods (Table 2).

In addition to direct deposits, key risk times for slurry spreading in the catchment are in the autumn and spring. To account for slurry spreading contribution to *E. coli* store in this catchment, *E. coli* store on grassland between 31 January and 1 April is assumed to be 2.1 × 10^8 CFU per m^2, based on the findings of McGechan and Vinten (2003).

E. coli detachment or washout rate from each cell at each timestep (t) during rainfall events is estimated based on the method of Collins and Rutherford (2004), applied here at hourly resolution.

$$Z,t = C_p \frac{O,t}{T_r} \ (when\ O,t\ <\ T_r) \quad (2)$$

$$Z,t = \ C_p \ (when\ O,t \geq T_r) \quad (3)$$

Where Z,t is the *E. coli* detachment or washout rate (*E. coli*/hr) during the timestep, O,t is the cell surface runoff rate (mm/h) during the timestep (from the surface runoff model) and T_r is threshold a runoff coefficient, taken as 1.04 mm/hour (Collins and Rutherford, 2004). C_p is the available *E. coli* store (E_x), modified by a calibration constant (K_1), discussed further in Section 3.5.

$$C_p = E_x K_1 \quad (4)$$

The calculated travel time from each high-risk cell is calculated based on the surface runoff model for each model time step. This is then used to route *E. coli* load at each hourly timestep from each cell (Z,t) to the outlet of the catchment. Time series of river flow based on the hydrological model (Q,t, m^3/s) and total *E. coli* load in surface runoff (*E. coli*/m^3) can then be used to determine concentrations water arriving at the outlet of the catchment from field sources. Thus, the concentration of *E. coli* from diffuse runoff field sources at each model time step ($E.coli_F, t$), can be expressed as:

$$E.coli_F, t = \frac{\sum (Z,t)}{(Q,t)} \quad (5)$$

Table 1
Bovine and ovine die-off constants (*b*) for different seasons, from Avery et al. (2004) and Oliver et al. (2009).

Season	Bovine die-off constant (day^{-1})	Ovine die-off constant (day^{-1})
Autumn/winter	0.0606	0.0640
Spring/summer	0.0909	0.0920

Table 2
Catchment livestock densities, total grassland area (from DEFRA County level data), deposit data and assumed grazing periods in the catchment (based on Oliver et al., 2009, Oliver et al., 2018).

Livestock type	Livestock Count – County level	*E. coli* (CFU) contribution per livestock	Ein_x *(CFU)* per 5 m^2 of grassland	Grazing period
Dairy cow	9682	8.99×10^8	85,195	1 Apr–31 Oct
Beef cow	17,360	2.54×10^9	431,602	1 Apr–31 Oct
Calves	23,644	2.10×10^{10}	4,662,237	1 Apr–31 Oct
Sheep	151,061	7.74×10^8	968,452	1 Jan–14 Apr[a]; 1 May–31 Dec
Lambs	127,827	1.01×10^{10}	14,934,373	1 May–1 Nov
Grassland total (ha)	51,081			

[a] removed for lambing.

2.5. SSO spill volumes, loading and routing

SSO monitoring equipment has recently been installed within the catchment as part of the current commitment to provide event duration monitoring data of all operational SSOs to the UK public (Environment Agency, 2023). In the study catchment, spill event durations are currently estimated based on monitored level data within chambers connected to outflow pipes (discharging to surface waters), with start and stop times logged as when water level exceeds the outflow weir crest/pipe invert level. Although monitoring systems are not designed to estimate volumes or pollutant loadings to receiving waters, a simple approach is proposed to make estimates of flow rate and loadings based on sensor information.

Raw water level data (collected via ultrasonic probes) at 15 min resolution data is provided at each of the 20 SSO sites within the catchment (Fig. 1). Based on asset data (weir/pipe dimensions) and monitored level information for the analysis period, SSO spill volumes at each site are calculated every 15 mins where the water level exceeds the outflow weir crest or pipe invert level based on standard equations for hydraulic structures and pipe flows. A similar approach has been used by Fachs et al. (2008) to estimate flow rates from urban drainage systems overflows.

At sites where the outflow is controlled by a weir, the SSO spill flowrate at each site ($Q_{spill,x}$, m^3/s), is calculated every 15 min as:

$$Q_{spill,x} = \frac{2}{3} C_{dw} L \sqrt{2g} h^{\frac{3}{2}} \quad (6)$$

Where C_{dw} is the coefficient of discharge for a weir, taken at 0.6. L is the effective length of weir (m), g acceleration due to gravity (m/s^2) and h is the height of water surface above weir crest (m). For sites where the outflow is controlled by a pipe, two states are simulated to consider when the pipe is surcharged or flowing with a free surface, defined at each time step by the monitored water level relative to the pipe soffit level. When the pipe is in surcharged condition, the spill flowrate is

calculated based on an orifice condition:

$$Q_{spill,x} = C_{do} a_o \sqrt{2gh} \quad (7)$$

Where a_o (m^2) is the area of the orifice and h (m) is the height of water surface above the outlet. Where C_{do} is the coefficient of discharge of the orifice, taken at 0.57. When the flow in the pipe has a free surface, the flow rate is based on Manning's equation:

$$Q_{spill,x} = \frac{1}{n} \frac{A^{\frac{5}{3}}}{P^{\frac{2}{3}}} S_o^{\frac{1}{2}} \quad (8)$$

Where A is the cross-sectional area of the portion of the channel occupied by the flow (m^2), n is the Gauckler–Manning coefficient (s/[$m^{1/3}$]), taken as 0.014 for vitrified clay, P is the wetted perimeter of the channel occupied by the flow (m), S is the pipe slope (based on asset data). Eq. (6) assumes that the flow in the pipe is uniform, whilst unlikely to be the case the short duration of free surface pipe flow conditions in most cases means that the uncertainty arising from this assumption is unlikely to be significant. The total spill volume per hourly timestep ($V_{spill,x,\ t}$) at each SSO is calculated by the integration of the calculated flowrates. Currently there is no sampling of *E. coli* of storm overflow sites to estimate loadings within SSO spill volumes. Therefore for the purposes of this application *E. coli* concentrations of 40,000 *E. coli* (CFU)/100 ml have been utilized based on the previous observations found in literature (Ellis and Yu, 1995; García-García et al., 2021; Hamel et al., 2016; USEPA, 2008) to calculate the *E. coli* load from each SSO (SSO_x,t). The implications of this assumption are discussed further in Section 4.

As point source discharges, loadings from SSOs are subject to considerable dispersion effects within the receiving water (Rutherford, 1994). To account for this, SSO loadings from each site at each timestep are routed to the catchment outlet using an Aggregated Dead Zone (ADZ) transport and mixing model (Beer and Young, 1984; Wallis et al., 1989). The ADZ is a simple two parameter routing approach which accounts for mixing processes within surface waters. Unlike the (more commonly used) Advection Diffusion Equation the ADZ accounts for skewed distributions commonly observed during mixing studies conducted in surface waters (Rutherford, 1994). The ADZ model provides loadings at the downstream catchment outlet from each individual SSO site (SSO_{Dx},t) as:

$$SSO_{Dx}, t = -\alpha(SSO_{Dx}, t-1) + (1+\alpha)(SSO_x, t-\delta) \quad (9)$$

Where $\alpha = -e^{\left(\frac{-\Delta t}{\bar{t}-\tau}\right)}$ and $\delta = \frac{\tau}{\Delta t}$. The parameter $\bar{t}$ is mean traveltime over the reach (s) and τ is an initial reach time delay (s). The two ADZ parameters ($\bar{t}$, τ) can be expressed as the dispersive fraction (D_f), as defined by Young and Wallis (1986), and used to scale the mixing effects within a reach.

$$D_f = \frac{(\bar{t} - \tau)}{\bar{t}} \quad (10)$$

To deploy the ADZ model to each SSO spill, the mean reach travel time ($\bar{t}$) is estimated based on the surface runoff model described in Section 2.3. By applying a series of uniform rainfall events (from 0.08 to 1 mm/hr) over the catchment, travel time against catchment outlet river flow relationships for each SSO were extracted from the hydrological model. In each case a uniform rainfall intensity was applied to the catchment until the modelled river flow at the outlet stabilized. This allowed representative mean travel times ($\bar{t}$) from each SSO to be determined over a range of measurable catchment flow conditions (from 6.21 - 79.57 m^3/s), based on the coordinates of each SSO as identified based on asset records and identified river distance (Table 3). As the time delay parameter (τ) cannot be directly established by the hydrological model, τ is calculated for each timestep and SSO based on the traveltime (from above), according to Eq. (10). In this case a fixed value of $Df = 0.2$ is taken in all cases, based on the database values of dispersive fractions from UK rivers found in Guymer (2002). Given the uncertainty induced by the use of a single representative Df value, a sensitivity analysis of this parameter on SSO predictions was also carried out (see Section 4.3). Routed *E. coli* loadings from each SSO are summed for each model timestep and diluted by the calculated river flow volume at the catchment outlet to determine the SSO *E. coli* component ($E.coli_S, t$) of the model (Eq. (11)). Similarly to the diffuse component, a calibration parameter (K_2) is also applied, discussed further in Section 3.5.

$$E.coli_S, t = K_2 \frac{\sum_{x=1}^{x=20} (SSO_{Dx}, t)}{(Q, t)} \quad (11)$$

Table 3
Characteristics of Leam catchment SSOs included in *E. coli* model, based on monitored period between April 2021 - March 2023. EA EDM data is the sum of the annual return data in 2021 and 2022.

Name	River distance to sampling site (km)	Modelled traveltime under 1 mm/hr unform rainfall (h)	% of total spill volume in catchment	EA EDM return -Total Duration '21 and '22 (hrs)	Outflow control type
SSO_1	4.40	7	65.7	2857.7	Pipe
SSO_8	15.45	21	5.0	37.5	Pipe
SSO_{12}	21.24	29	6.0	782.1	Weir
$SSO_{19.1}$	29.14	35	9.7	3086.8	Pipe
$SSO_{19.2}$	29.14	35	3.5	371.6	Pipe

3. Model input data, water quality sampling and calibration

3.1. Rainfall and river flow

Radar rainfall at $1km^2$ spatial resolution, 15 min temporal resolution, used as field runoff model input, was acquired from the UK met-office's NIMROD system. Rainfall was aggregated into hourly intervals to be used with the runoff generation and pollutant wash-off components of the model. A set of rainfall events was selected for validation of the hydrological component of the field runoff model (Table 4). Summary of the statistics for the four events used for the diffuse component of the *E. coli* model (calibration and validation) are provided in Table 6.

River flow (m^3/s) data from a flow gauging station situated at the outlet of the study catchment was obtained from the UK EA (NRFA 2023). It was used as initial baseflow input for field runoff model and for the validation of the hydrological model.

3.2. Land use

UKCEH Land Cover® plus: Crop maps were used to create an *E. coli* high-risk area map. In this case, grasslands were selected due to livestock grazing throughout most of the year, creating *E. coli* stores that replenish and die off with time (as described in Section 2.4). Fig. 1 shows

Table 4
Summary of rainfall events used to re-evaluate the surface runoff model. Quoted durations are based on presence of rainfall at any position in the catchment. Intensities are based on temporal and spatial averaged values. Initial and peak flow rates during each event based on EA gauging station data.

Event No.	Start date	Duration	Rainfall intensity (mm/hr)		River flow data	
			Average	Peak	Initial flow (m^3/s)	Peak flow (m^3/s)
A1	03.12.2021	8h	1.10	2.10	5.45	19.2
A2	03.03.2021	15h	0.72	2.33	2.02	7.72
A3 (= E1)	04.12.2020	16h	0.71	1.48	0.43	5.85

the distribution of grasslands in the catchment during the study period.

3.3. Storm sewer overflow data

Monitored Storm Sewer Overflow Data (water level time series from 20 catchment SSO's) and asset location data was obtained from the local water utilities Event Duration Monitoring (EDM) analytics platform. An initial screening of the calculated volume from each SSO site (based on Eqs. 6-8) was performed. This showed that 5 out of the 20 SSOs contributed approximately 90 % of the total spill volume/load over the 24 month study period (April 2021 – March 2023). Therefore, to simplify the model and further analysis, calculated catchment SSO loadings included only these 5 SSOs. Information on each of these SSO's is included in Table 3, alongside nationally published EDM return data (Environment Agency, 2023). Calculation of traveltimes to the abstraction site is based on the application of the hydrological model and SSO location (river distance to sampling site)

3.4. Water sampling (E. coli data)

Water samples were taken from the River Leam at the water abstraction site using autosamplers during and shortly after four monitored rainfall events in the catchment. This enabled the continuous collection of hourly/bihourly water samples during storm runoff events, which successfully captured the short-term fluctuations of *E. coli* concentrations at the abstraction site. The auto-samplers were manually triggered before the arrival of forecasted rainfall events. For each event sampling was carried out for a period of 1–5 days, which enabled the acquisition of water samples during the full surface runoff period following the rainfall events. During the sampling campaign a range of seasonal conditions and rainfall events of varying intensity and duration were captured over the period from September 2021to February 2023 (Table 6).

During each event, designated compartments within the autosamplers were filled with ice to keep the adjacently stored collected sample temperature low and stable. Samples were placed in a controlled environment (3–5C°) within 12 h and analysed within 24 h of collection. The samples were analysed using Total coliforms and *E. coli*- Isolation and Enumeration from Water by Membrane Filtration method as stated in The Standing Committee of Analysts (2016) based on Sartory and Howard (1992). The water sample is filtered through a cellulose acetate membrane filter upon which bacteria are entrapped. The filter is then placed on a selective growth medium and incubated at 30ºC ± 1.0ºC for 4 ± 0.25 h followed by 37ºC± 1.0ºC for 17 ± 3 h. After incubation is complete the colonies, which are characteristic of Coliforms, and Escherichia coli are counted. For further details regarding the sampling and data quality assurance procedures see Suslovaite (2023).

3.5. Model calibration

Understanding *E. coli* loadings within surface waters is subject to considerable uncertainty. Whilst information concerning the arrival and duration of microbiological loadings into river systems can be directly characterized using monitoring or input data from rainfall radar or SSO sensors, due to a lack of direct monitoring of loadings within field runoff and storm overflows, the model utilizes literature values. However, it is known that these values can be highly variable between sites and with time (Madoux-Humery et al., 2015). Further to this, to maintain a simple model structure, processes such as *E. coli* decay/die off in the river network are neglected. To mitigate this, two calibration parameters (K_1, K_2) are introduced to scale loadings from field runoff and SSOs respectively. It should be noted that these parameters are used to adjust magnitude of *E. coli* loadings and do not affect the arrival times and durations of *E. coli* events (i.e. the primary model application). Calibration of the model is based on initial monitored event (E1), and then validated on the remaining 3 events (E2–4). The sampling events are distributed over the year to cover a range of seasonal and hydrological conditions (winter and summer, with initial to peak river flows ranging well over the Q70 to Q10 range over the 4 events), with rainfall durations ranging from 8 to 41 hrs. This provides some indication of the scale of uncertainties to be expected if the processes approximated by the calibration parameters are assumed to be constant throughout the year.

4. Results and discussion

4.1. Surface runoff model

A set of events chosen for the validation of the hydrological component of field runoff model are listed in Table 4. Event A3 is also used to calibrate the *E. coli* model (event E1). Spatial distribution of temporally averaged rainfall for events A1 and A2 can be seen in Fig. 2, event A3's rainfall can be seen in Fig. 4 under event E1.

The results of hydrological model calibration and validation can be seen in Fig. 3 with the performance statistics listed in Table 5. The performance of the surface runoff model was evaluated over the duration of the hydrograph (T) using R-Squared (R^2), Volume Conservation Index (VCI, Eq. 12), model efficiency coefficient (Eq. 13) and prediction error in the time to peak (ΔTp).

$$VCI = \sum_{t=0}^{T} Q, t_{model} \Big/ \sum_{t=0}^{T} Q, t_{observed} \tag{12}$$

$$E = 1 - \frac{\sum_{t=0}^{T} (Q, t_{model} - Q, t_{observed})^2}{\sum_{t=0}^{T} (Q, t_{observed} - \overline{Q, t}_{observed})^2} \tag{13}$$

In Asfaw et al. (2018), VCI ranged between 0.82 and 0.99 compared to between 0.84 and 1.06 here. Further the ΔTp range of 1–5 hrs was reduced to 1–3 hrs during this validation. While the efficiency coefficient has seen a reduction (from a range of 0.83 - 0.91 to 0.63 - 0.88), overall the error statistics show the hydrological model to still be valid and suitable to use as a basis for travel time estimation.

4.2. Measured E. coli dynamics and model performance

The *E. coli* sub models (Eqn 5 and 11) were calibrated and validated using a set of rainfall events and the related statistics are listed in Table 6. Initial and peak river flow measured at the gauging station are also provided. For each event, the estimated rainfall depth for an equilivent duration 1 year return period (RP) storm has been calculated using the recent UKCEH FEH 22 model (UKCEH, 2023; Vesuviano, 2022). The events used for model validation and calibration are well within the 1 year return period, and are therefore reasonably typical in terms of overall magnitude. Event E1 was used for calibration of parameters K_1 and K_2 with the remaining 3 events utilized for validation. Following calibration, a value of 0.4 was used for both K_1 and K_2. Fig. 4 displays the spatial distribution of temporally averaged rainfall for each event. Fig. 5 presents the measured *E. coli* for each event, spatially averaged rainfall within the catchment, and the outputs of the *E. coli* models. The SSO, field and combined (i.e., summation of SSO and field components) model outputs are presented.

Table 7 presents goodness of fit statistics for the combined *E. coli* forecasting model for each event. ΔA (hrs) - prediction error of first arrival time, ΔD (hrs) - prediction error of event duration, ΔTp (hrs) - prediction error of time to peak.

Table 8 presents the calculated total *E.coli* load at the Leam abstraction point over each event from field, SSO and combined sources.

For all events, observed and modelled *E. coli* exhibit large rises in the sampling period following rainfall. Although the forecasted peak durations are over predicted at times, these deviations are in the order of a few hours and are a fraction of the overall storm durations. The model suggests that event E1 is characterized by significant contributions from

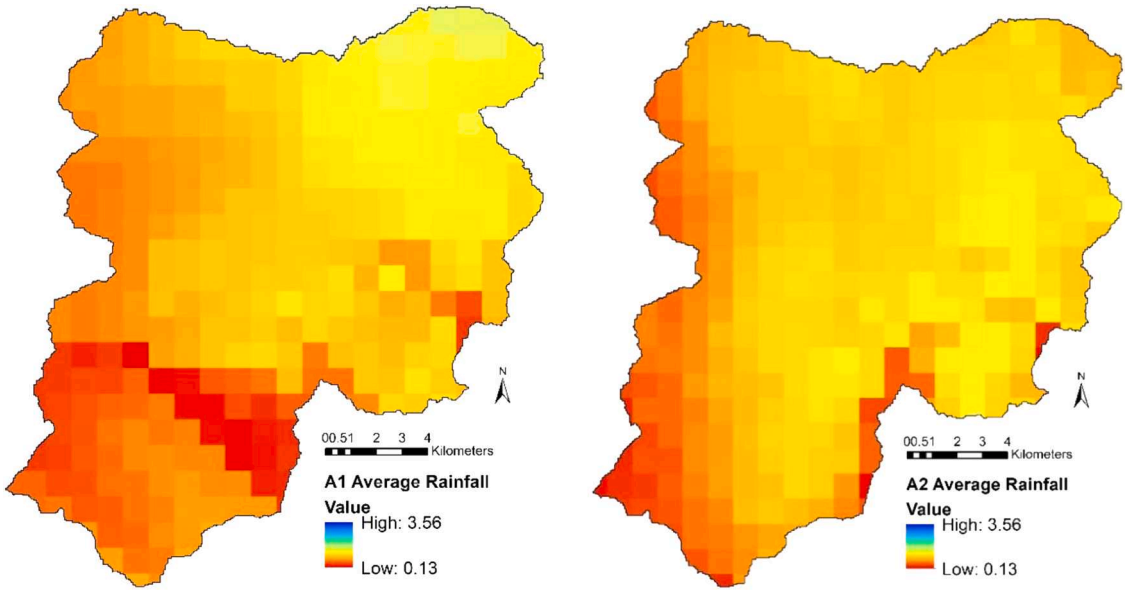

Fig. 2. Spatial distribution of temporally averaged rainfall (mm) for the events used in hydrological model validation.

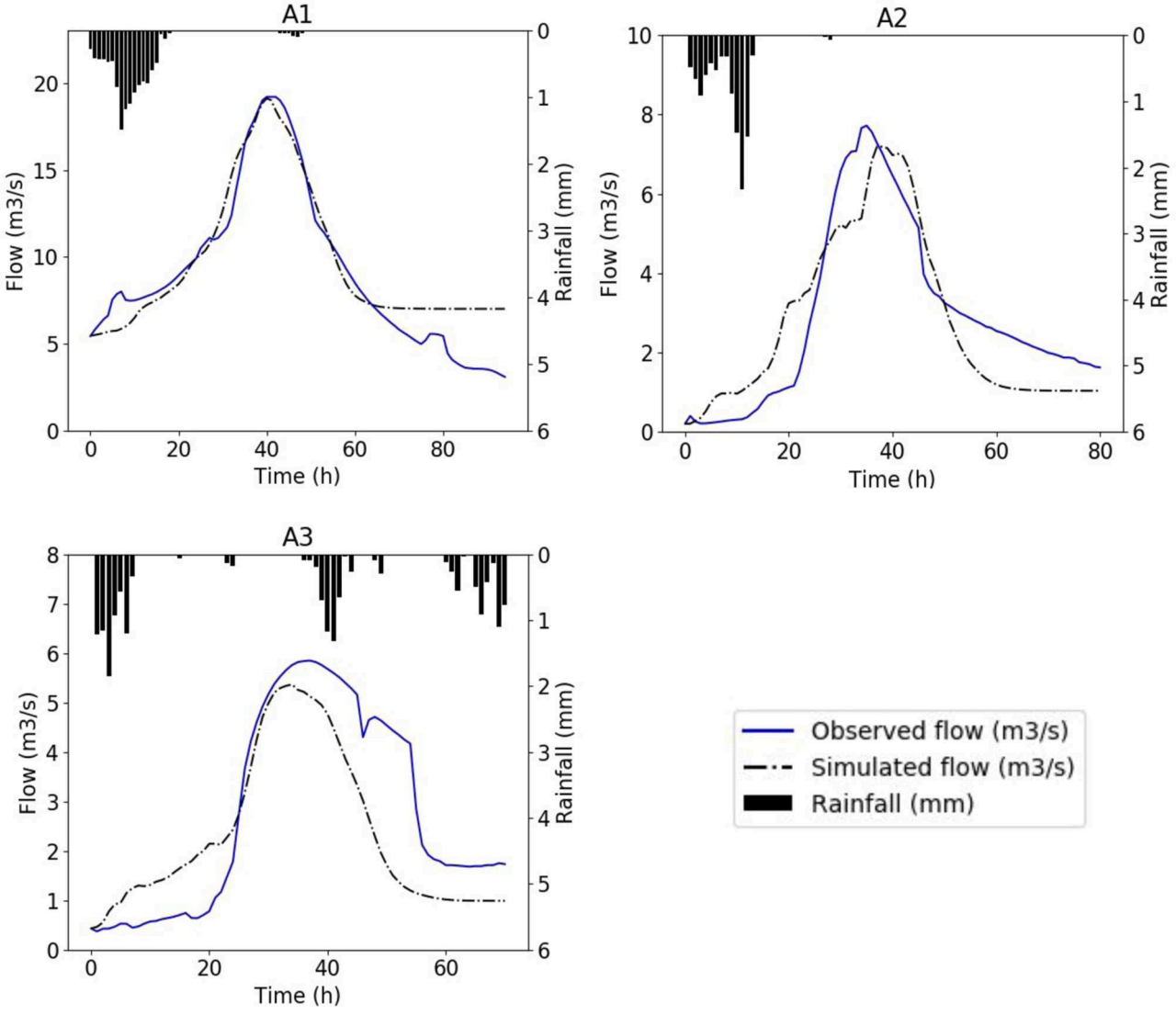

Fig. 3. Field Runoff hydrological model validation (modelled and predicted flow, spatially averaged catchment rainfall).

Table 5
Flow simulation model error statistics.

Event	R^2	E	VCI	ΔTp (hrs)
A1	0.90	0.88	1.06	1
A2	0.80	0.79	0.94	2
A3	0.68	0.63	0.84	3

both SSO and diffuse runoff sources. The SSO being responsible for the initial spike (due to the SSO spill from SSO_1 relatively close by the abstraction site), and the tail (from 20 to 60 h after sampling commenced) being due to the slower diffuse runoff. The preceding rainfall event is moderate and of 8 hrs duration, and sufficient to cause approximately equivalent loadings from both SSO and field runoff sources. Whilst this event is used for calibration, the model structure correctly predicts the arrival time and duration of the event.

The model prediction for event E2 significantly underestimates the arrival time of the *E. coli* peak concentrations; however, the end of the event is predicted reasonably well. In this case, the event is of lower intensity, but of longer duration, with a relatively high initial river flow. Hence, in this case predicted SSO volumes and loadings are significantly lower and the predicted *E. coli* contributions are mainly from diffuse runoff. The spatial distribution of rainfall intensity suggests a lower rainfall closer to the catchment outlet, and in this case, the model may be over predicting wash off from these areas leading to higher *E. coli* loadings at the start of the event than is observed.

Event E3 is an example of a high intensity, shorter duration event typical of summer rainfall with a low initial and peak river flow. In this case the model predicts that the runoff and loadings from field areas and corresponding diffuse pollution impacts are relatively minor, with the main source of pollution from SSOs which are more likely to overflow during the sudden inundation from such rainfall events. In this case the model gives a generally good estimation of the arrival time and overall duration of the observed *E. coli* concentrations. Two peaks are observed in both measured and modelled *E. coli* values, which are a result of inputs from SSOs at different locations in the catchment. The model predicts a longer duration initial peak than is observed and the arrival times for the second peak are overestimated by approximately 5 to 6 hrs. This discrepancy may be caused by residual errors within the hydrological model when predicting a short, flashy event, a lack of calibration of the mixing parameters within the routing methodology, or sensing errors within the SSOs themselves.

Event E4 is a prolonged and complex rainfall event resulting in multiple *E. coli* peaks and with significantly larger river flow rates than E1–3. Some SSO loading is present throughout the event but the majority of *E. coli* load supplied via diffuse sources from agricultural runoff. Despite the complexity of the event, the model gives a reasonable approximation of the arrival time of elevated E .coli levels commencing shortly after the initiation of sampling. Due to the length of the event, it is unlikely the sampling period covered the end of the event in this case.

The overall results suggest that the sampling campaign has captured events with a diverse range and a variation of sources (SSOs and field runoff). Despite the logistical challenges in measuring *E. coli* at high resolution, this demonstrates that value of measuring events over a range of seasonal conditions, such that relatively short summer rainfall events, as well as longer rainfall events in winter are captured. Further, sampling over winter and summer provides evidence that the model is fit for purpose over a good range of hydrological conditions, which is significant due to the influence of river travel time calculations on the model output.

4.3. Sensitivity analysis

Mixing and dispersion processes in rivers can have significant effects on arrival times and duration that pollutants remain over given thresholds (Camacho Suarez et al., 2019a). Given that the application of the model is to forecast arrival times and duration of *E. coli* peaks it is important to understand the uncertainty introduced into model outputs due to the lack of direct quantification of mixing processes, and associated use of standard literature values of mixing parameters. Based on the survey of UK rivers (Guymer, 2002), dispersive fraction commonly falls within the range $0.05 < D_f < 0.4$. Fig. 6 shows results of a sensitivity analysis carried out on the SSO *E. coli* model for event E3 based on these values as upper and lower bounds. At this site, the analysis shows a relatively small change in arrival and peak timings over this range of D_f, with a more significant effect on peak concentrations (Table 9). Given this result, it is likely that some improvements in model performance could be achieved in this case by calibration of dispersive fraction, with higher D_f values leading to earlier arrival times which may positively affect performance of events 1 and 3. However, at this site the use of a representative D_f value provides an acceptable level of model performance. In this case it is noted the most significant SSO (SSO_1) is relatively close to the catchment outlet (see Table 3), which may reduce the significance of the mixing processes. In other catchments, with more spatially disrupted SSO loadings results are likely to be more sensitive to the D_f parameter, and hence direct calibration may be required. Further understanding of mixing processes at sensitive sites may also be improved by undertaking solute tracing experiments.

4.4. Annual simulation of E. coli over Jan - Dec 2022

Whilst the primary objective of the work is to validate an event-based forecasting methodology for *E.coli* peaks under common rainfall events, it is also informative to consider the results from a yearly simulation of rainfall driven acute impacts and consider the relative modelled loading from different sources in the catchment. The full yearly record of spatially distributed rainfall as well as SSO water level data over the 2022 calendar year was therefore taken as model input with resulting time series outputs of modelled *E.coli* used to derive percentile values and relative loadings. It is important to note that the proposed approach does not model *E.coli* during dry weather/base flow conditions. Hence, for the purposes of this simulation *E.coli* concentrations in the absence of modelled loadings are taken as the mean of sampled measurements taken in dry weather flow conditions (395 CFU/100 ml based on 36 measurements).

Table 10 presents 90th percentile *E.coli* values resulting from the

Table 6
E. coli sampling event dates, durations, sampling frequencies, and associated catchment rainfall statistics. Estimated 1 year RP rainfall depths for each event duration are also provided based on the UKCEH web service. Initial and peak flow rates during each event based on EA gauging station data.

Event No.	Start date	Sampling duration and frequency[a] (hrs)	Catchment Averaged Rainfall Statistics				River Flow Data	
			Duration (hrs)	Depth (mm)	Peak intensity (mm/hr)	1 year RP depth (mm)	Initial Flow (m^3/s)	Peak Flow (m^3/s
E1(A3)	03.12.21	82 (2)	8	7.3	1.9	21.8	0.43	5.85
E2	05.02.22	114 (2)	32	10.7	1.3	31.6	0.72	2.53
E3	16.08.22	46 (2)	9	9.2	2.5	22.6	0.25	0.39
E4	12.03.23	68 (1)	41	11.5	1.5	33.6	0.29	2.30

[a] in brackets.

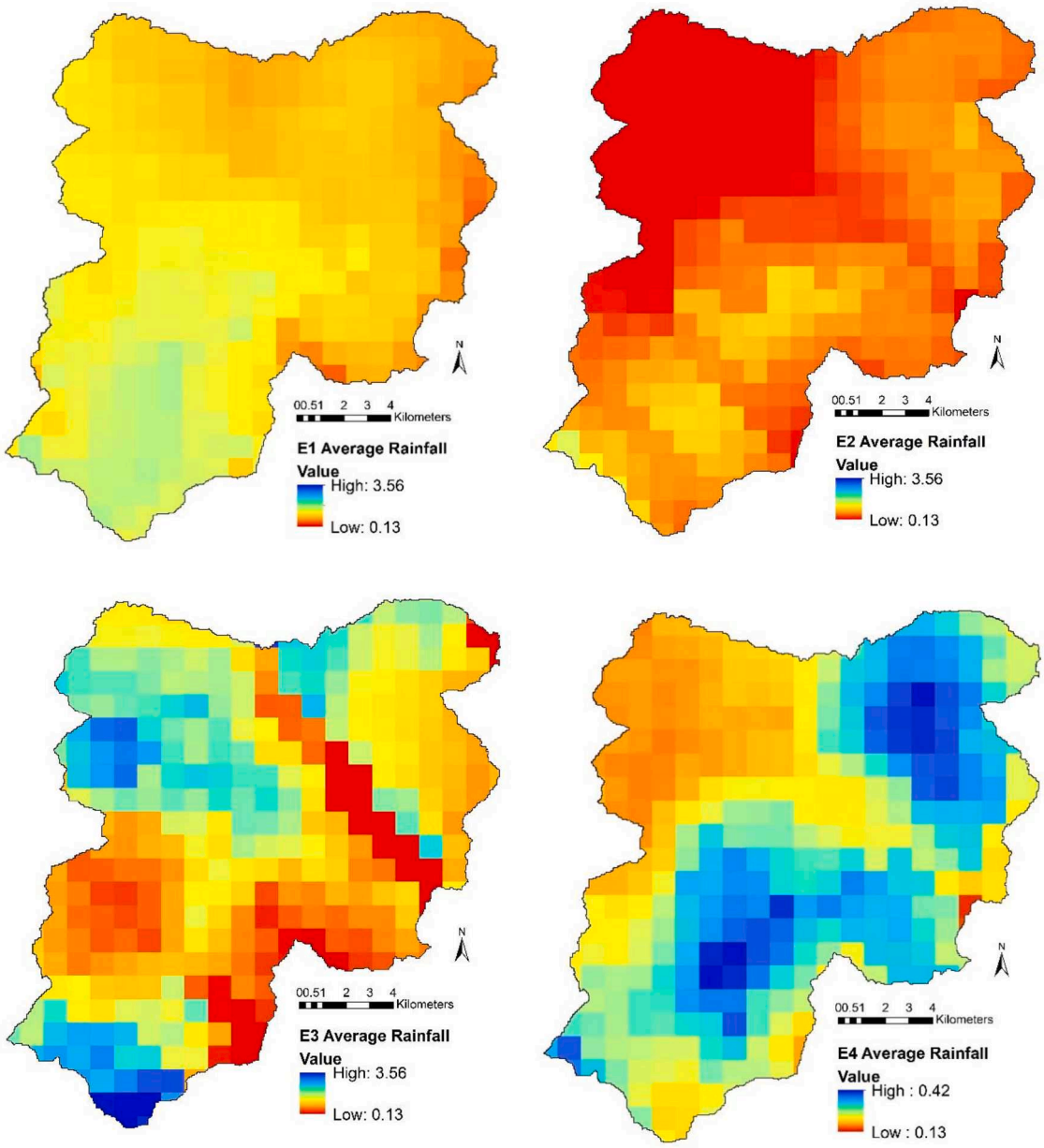

Fig. 4. Spatial distribution of temporally averaged rainfall (mm) for the events used in E. coli model calibration (E1) and validation (E2–4). Note E4 is plotted using an altered scale.

simulation, which may be considered in the context of current UK/EU bathing water standards (90th percentile of 900 CFU/100 ml for the minimum 'sufficient' classification (EU, 2006)). However, it should be noted that such assessments are based on a low number of sampled measurements (commonly 12–16 per year) conducted within the bathing water season only. To show relative contributions, results are presented in terms of the total *E.coli* as well as results from the separate field runoff and SSO *E.coli* sub models.

Results from the simulation show that the modelled water quality falls short of current bathing water standard classifications. Considering the full calendar year, contributions from both field and SSO sources are significant (with field runoff being marginally higher), and contributions from either source independently are sufficient to exceed the minimum bathing water threshold. It is notable that current official assessments based on infrequent measurements are unlikely to provide comparable results to a model considering short term dynamics in which runoff/SSOs causes *E.coli* to rise significantly after rainfall events.

Table 11 presents calculated total and apportioned *E.coli* loadings (CFU) over different seasons throughout 2022. To consider potential SSO mitigation (i.e. via the installation increased sewer storage or surface runoff mitigation), a simulation in which the contribution from SSO_1 (i.e. the most significant point source) is removed is also considered.

Table 11 shows that overall modelled field loadings are larger than SSO loadings in this catchment, although the relative significance changes over the year. Winter/spring seasons are dominated by larger and longer rainfall events causing significant field runoff volumes, increasing the relative loadings from diffuse sources above those from SSO's. This also corresponds to the period in which field loadings are assumed to be higher due to increased grazing and slurry spreading. In Summer/Autumn, rainfall volumes are lower with reduced field runoff. However, the increased proportion of low-duration high intensity rainfall events in summer (e.g. E3) increases the relative significance of SSO loadings in the catchment, as these events are still likely to cause spills

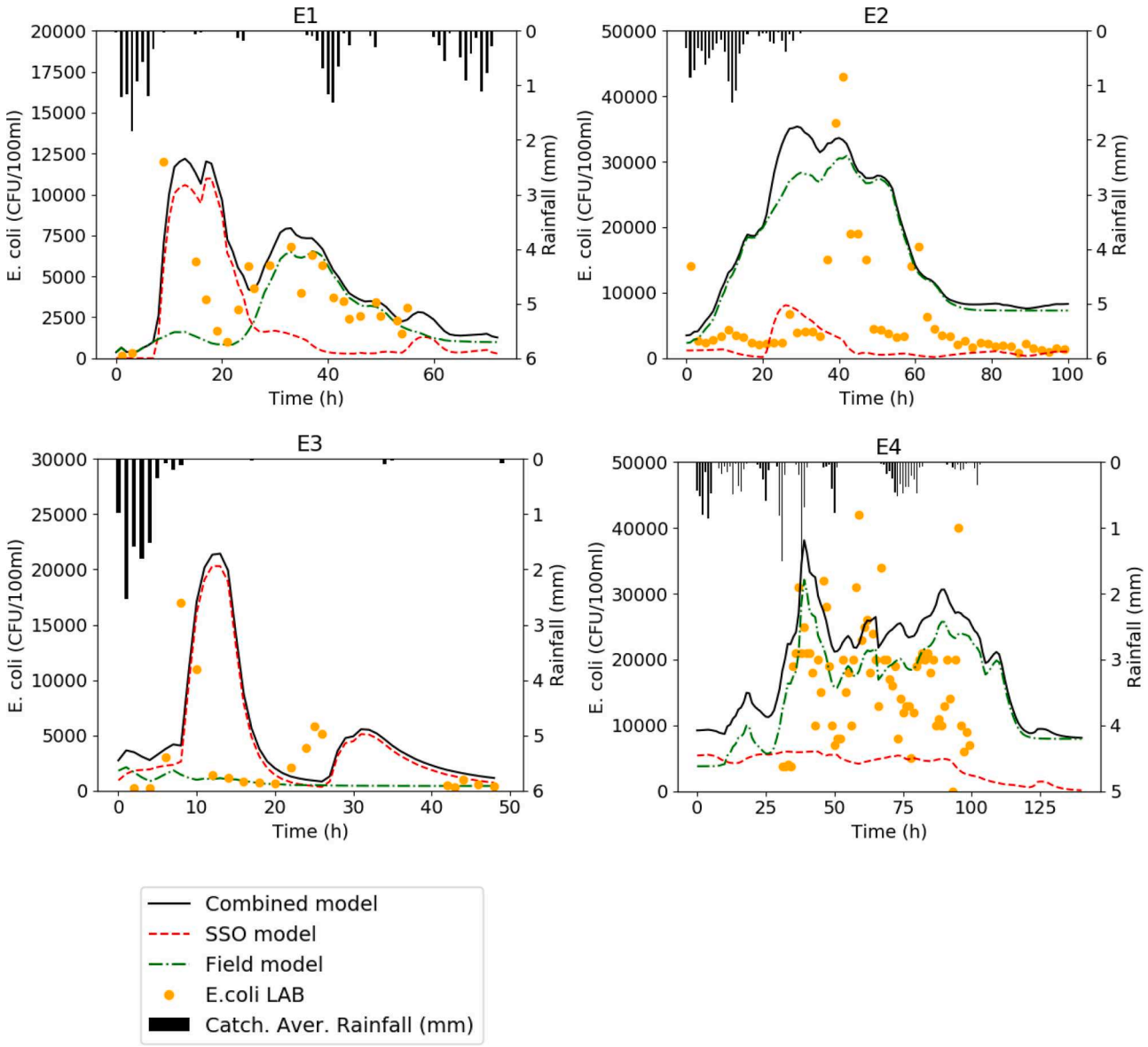

Fig. 5. Results of combined model and measured (LAB) E. coli data showing the contribution from the field runoff and SSO models and spatially averaged rainfall ($K_1 = 0.4$, $K_2 = 0.4$).

Table 7
Error statistics for combined *E. coli* model.

Event	ΔA (hrs)	ΔD (hrs)	ΔTp (hrs)
E1	2	2	7
E2	11	19	9
E3	1	1	4
E4	24	45	6

Table 8
Total calculated E.coli loads (CFU) over each event (combined and sub models).

Event	SSO CFU	Field CFU	Combined CFU
E1	1.07×10^{13}	2.75×10^{13}	3.82×10^{13}
E2	6.61×10^{12}	7.58×10^{13}	8.24×10^{13}
E3	2.51×10^{12}	4.20×10^{11}	2.93×10^{12}
E4	3.34×10^{13}	1.20×10^{14}	1.53×10^{14}

from urban drainage networks (Shepherd et al., 2023).

The removal of SSO_1 contribution from the simulation has resulted in reduction of total bacterial loads throughout the year. Notably, the largest reduction was forecasted between the months of October to December. Therefore, the significance of this SSO as *E. coli* source in the catchment is further reiterated by the results of the annual simulation.

5. Discussion

Similar to past studies of which collected high resolution measurements of FIOs in surface waters following precipitation (e.g. Hellweger and Masopust, 2008; Oliver et al., 2015), all four events monitored in this work exhibit significant (order of magnitude) increases in observed *E. coli* after moderate (< 1 year return period) rainfall events. This supports past work which has called for enhanced monitoring and/or modelling of microbial water quality for regulatory classification of waterbodies and/or health risk assessment (Zan et al., 2023). Current characterization of waterbodies for EU/UK bathing water assessments can be based on as few 12 samples per year (EU, 2006), such sampling is highly unlikely to effectively characterize the effects of rainfall driven

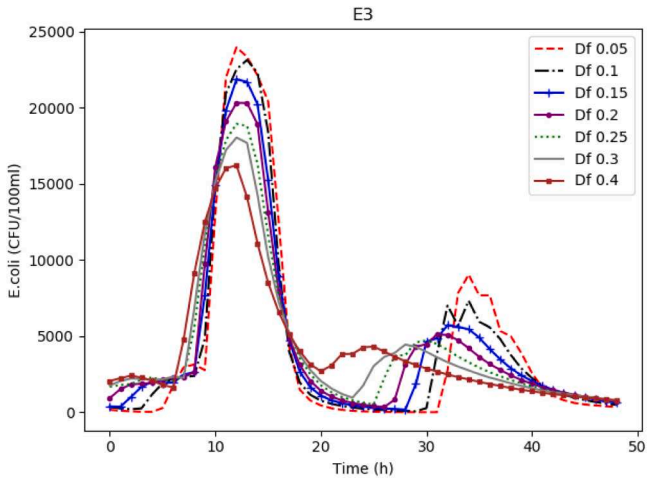

Fig. 6. Sensitivity of SSO model to dispersion fraction (*Df*) parameter for event E3.

Table 9
Difference in arrival, peak times and concentrations for E3 in relation to $Df = 0.2$ (assumed value).

Dispersive fraction (*Df*) value	Difference in arrival time (hrs)	Difference in peaks (hrs)	Difference in peak *E. coli* concentrations (CFU/100 ml)
0.05	1	0	3700
0.1	0	1	2800
0.15	0	0	1500
0.2	0	0	0
0.25	−1	0	−1300
0.3	−1	0	−2300
0.4	−2	0	−4100

Table 10
Forecasted 90th percentile concentrations over 1st Jan - 31st Dec 2022 based on combined (Total) and sub-models.

Total (CFU/100 ml)	Field Only (CFU/100 ml)	SSOs Only (CFU/100 ml)
7726	3679	3242

impacts which can vary significantly at sub daily timescales.

Whilst increases in faecal pollution after rainfall events are expected, this study has also considered how the duration and distribution of elevated periods of *E. coli* can be better understood by the characterization of sources, hydrological pathways and travel times facilitated by the use of spatially distributed rainfall, land use and distributed monitoring at SSOs. For example, where field runoff combines with significant SSO spill contributions (as suggested during event E1) multiple distinct peaks are observed. This supports previous evidence that at this spatial scale the characterization of the spatio-temporal hydrological response of the catchment and the associated pollutant sources, pathways and dilution potential is significant when aiming to model acute impacts (Asfaw et al., 2018; Neill et al., 2020). I.e., rainfall events with similar return periods, but with varying spatial and temporal distributions may result in significantly different pollutant responses due to the distribution and characteristics of source areas across the catchment and associated travel times, hydrological pathways as well as the assimilative capacity of the receiving water (dilution). For *E. coli,* this includes consideration of both the distribution and density of livestock (Oliver et al., 2018; Neill et al., 2020), but also the variations in condition and performance of sewer networks (and associated SSO's) which may be affected by localized factors such as network blockages and sewer maintenance (Shepherd et al., 2023). In general, shorter more intense events (e.g. such as in E3) may tend to have more significant relative contributions from SSOs as the higher insensity rainfall has the potential to exceed the capacity of urban drainage networks. Longer, less intense events (e.g. E4) see higher realtive contributions from field runoff sources (Camacho Suarez et al., 2019b). Considering the variation in the relative contributions of different sources over the duration of a rainfall runoff event may also be significant for when designing future studies considering microbial source tracking techniques for source identification (e.g. Wiesner-Friedman et al., 2022).

The proposed model developed in this work is developed with the intention of describing acute, rainfall driven events for forecasting applications such as short-term water resource management (Yassin et al., 2021) or bathing water alerts (Seis et al., 2018). To enhance practical application, it is also desirable to minimize required data collection beyond existing datasets which are available to water infrastructure operators via remote and/or distributed sensing. As such the model neglects several processes more relevant to understanding longer term/background pollution levels such as groundwater flow, sediment/water interactions and in stream microbial processes (e.g. Afolabi et al., 2023; Jiang et al., 2023) and utilizes literature values to characterize sources (which are effectively modified during model calibration). A key innovation of this work is the characterization of SSO impacts utilizing spatially distributed water level monitoring. Whilst traditional integrated catchment models characterize sewer impacts using complex sewer network models, these require extensive sewer asset records, detailed calibration and frequently suffer from high levels of predictive uncertainties in the prediction of spill volumes (Srivastava et al., 2018) and pollutant loads (Moreno-Rodenas et al., 2019). It is important to recognize the quantification of loadings by such means is subject to measurement errors (as well as further uncertainties associated with the calculation of flow rate, Leonhardt et al., 2014). Further work is required to better quantify such uncertainties as the direct monitoring of catchments is likely to increase in the future, with further potential to integrate modelling tools and live sensor data to overcome traditional challenges associated with modelling water quality in complex catchments.

Despite simplifications, results from the validation events suggest that expected peak *E. coli* magnitudes are predicted reasonably well by the proposed modelling approach. The calibrated model parameters K_1 and K_2 are both lower than unity, suggesting that initial source loading values used in this work may overestimate the *E. coli* burden in this catchment from both field and SSO sources. It is noted that the use of constant calibration parameters is a relatively simplified approach to account for uncertainties associated with source loadings and the omission of a number of complex microbiological processes from the model structure (e.g. in stream *E. coli* die-off). However, in this 300km^2 mixed use catchment, the model accuracy is adequate to provide useful

Table 11
Forecasted total loads over 2022 and catchment averaged rainfall depth.

	Rainfall depth (mm)	Total Load (CFU)	SSO Load (CFU)	Field Load (CFU)	Total without SSO_1 (CFU)
Jan-Mar 2022	130	2.05×10^{15}	1.73×10^{14}	1.87×10^{15}	1.94×10^{15}
Apr-Jun 2022	116	5.03×10^{13}	1.76×10^{13}	3.27×10^{13}	4.29×10^{13}
Jul-Sept 2022	83	2.70×10^{13}	1.37×10^{13}	1.32×10^{13}	2.12×10^{13}
Oct-Dec 2022	219	2.68×10^{14}	1.65×10^{14}	1.04×10^{14}	1.46×10^{14}
Full year 2022	548	2.39×10^{15}	3.69×10^{14}	2.02×10^{15}	2.15×10^{15}

information to the utility operator regarding likely peaks and durations of acute *E. coli* impacts arriving at the water abstraction site. As expected, some residual errors are present in the predictions, and overall there is a tenancy to overestimate the duration of *E. coli* peaks. As the model outputs are sensitive to travel time predictions, further refinement of the underlying hydrological model has the potential to improve performance (specifically calculated arrival time and peak durations), and further enhancement to the SSO model make be achieved by a direct calibration of the dispersive fraction parameter. However, given typical uncertainties in the measurement of *E. coli* itself (Harmel et al., 2016), as well the limited number of measured events, in this case it was considered preferable to avoid risks associated with over parameterizing or over-calibrating the model (e.g. see Beven, 2006).

Analysis of model outputs over the 2022 calendar year has demonstrated the relative contribution of field and SSO sources, with both having significant contributions in this mixed-use catchment. It is notable that relative contributions change over the seasons due to the nature of the rainfall events and the changes in field source loading due to agricultural activity. There is therefore potential further use of the model to explore potential mitigation options (i.e. simulating the effects of reducing field runoff, or reducing SSO spill volumes). However, it is recommended that further validation of the model is undertaken over a greater range (magnitude) of storm events to provide increased confidence that the size as well as duration of peaks can be predicted during more significant events (i.e. up to a 1 year return period).

For transfer to larger, more complex catchments (e.g. for those with longer timescales, or with significant WWTW impacts), the model may require further development to account for these processes and additional calibration. However, in smaller catchments a relatively simple model structure appears sufficient given the model application. This reduces calibration requirements and hence costs for model setup, which can be a significant burden for water quality models (Tscheikner-Gratl et al., 2019). In more complex catchments, a potential option is to integrate travel time-based modelling approaches and high resolution measurements with microbial source tracking techniques (e.g. Zan et al., 2023), to provide enhanced identifiability and validation of travel times from the variety of source areas.

6. Conclusions

This paper presents a novel approach to forecasting *E. coli* dynamics in surface waters under commonly occurring, acute rainfall events. To the best of the authors knowledge, no other validated methodologies are currently available in the scientific literature for the description of short term *E. coli* dynamics in mixed catchments (featuring significant diffuse and urban point sources) at comparable scales, utilizing equivalent input datasets. The methodology is based on the determination of travel times from source areas based on hydrological routing, radar rainfall and the novel use of distributed SSO water level monitoring and as such does not require the setup and calibration of a detailed high order hydrodynamic model of the river system or sewer networks. As the primary application is the forecasting of arrival times and durations of periods of elevated *E. coli* levels, understanding travel/arrival times is of primary importance, with factors that control the overall magnitude of *E. coli* peaks of secondary importance. As such, in the absence of monitoring data characterizing catchment source loadings, the methodology is based on assumed concentrations which are calibrated based on model outputs. Despite simplifications, the model provides a reasonably good representation of *E. coli* dynamics in most cases, with calibration parameters not varying significantly over the study period. This suggests the value in accounting for the temporal and spatial variability of sources (diffuse and SSO) when accounting for *E. coli* dynamics, particularly over short time periods in the order of hours. Further, the work provides a new demonstration of how distributed sewer monitoring and rainfall data can be utilized for water resource and surface water management. As the approach is not dependant on complex integrated hydrodynamic modelling and/or direct measurement of source loadings, it has potential to be deployed to water resource management applications such as water abstraction management and bathing water quality forecasting in real time.

The results from the monitoring campaign show significant differences in *E. coli* dynamics between the four monitored events as a function of spatial and temporal rainfall variability causing mobilization of different sources. This finding demonstrates the value of source characterization using remote sensing and spatially disturbed sensors and the significance of spatially distributed runoff. The proposed modelling approach can also be used as a source apportionment tool as it allows the effects of different sources to be disaggregated. Further work may consider identifying the significance of individual SSOs or field areas on high *E. coli* periods over longer timescales.

There is significant scope for development to identify and reduce modelling uncertainties, in particular, in larger more complex catchments it is likely that the model complexity will need to be increased to account for additional processes which are less significant in this case (e.g. *E. coli* die off). However, this effort would likely increase the number of datasets required for robust model calibration to overcome parameter identifiability issues. In this initial application, a simple model structure is preferred given the proposed application.

Declaration of Competing Interest

The authors declare the following financial interests/personal relationships which may be considered as potential competing interests:

Vaida Suslovaite reports financial support, equipment, drugs, or supplies, and writing assistance were provided by Severn Trent Water Ltd. Vaida Suslovaite reports financial support was provided by Engineering and Physical Sciences Research Council.

Data availability

The authors do not have permission to share data.

Acknowledgements

This work was funded by an EPSRC CASE award (EP/R513313/1, studentship no. 2282601) together with Severn Trent Water Ltd. We would like to thank the Severn Trent Water staff at Church Wilne microbiology laboratory for providing assistance in the analysis of river water samples.

References

Afolabi, E.O., Quilliam, R.S., Oliver, D.M., 2023. Persistence of *E. coli* in streambed sediment contaminated with faeces from dairy cows, geese, and deer: legacy risks to environment and health. Int. J. Environ. Res. Public Health 20, 5375. https://doi.org/10.3390/ijerph20075375.

Asfaw, A., Maher, K., Shucksmith, J.D., 2018. Modelling of metaldehyde concentrations in surface waters: a travel time based approach. J. Hydrol. 562, 397–410.

Avery, S.M., Moore, A., Hutchison, M.L., 2004. Fate of Escherichia coli originating from livestock faeces deposited directly onto pasture. Lett. Appl. Microbiol. 3, 355–359.

Bathing Water Regulations (2013) https://www.legislation.gov.uk/uksi/2013/1675/contents/made (Accessed at 08.06.2023).

Beer, T., Young, P.C., 1984. Longitudinal dispersion in natural streams. J. Environ. Eng. 109 (5), 1049–1069.

Beven, K., 2006. A manifesto for the equifinality thesis. J. Hydrol. 320 (1–2), 18–36. https://doi.org/10.1016/j.jhydrol.2005.07.007. ISSN 0022-1694.

Boehm, A.B., Soller, J.A., 2020. Refined ambient water quality thresholds for human-associated fecal indicator HF183 for recreational waters with and without co-occurring gull fecal contamination. Microb. Risk Anal. 16 (100139) https://doi.org/10.1016/j.mran.2020.100139. ISSN 2352-3522.

Brannan, K.M., Mostaghimi, S., Dillaha, T.A., Heatwole, C.D., Wolfe, M.L., 2002. Fecal Coliform TMDL for Big Otter River, Virginia: a case study. In: Total Maximum Daily Load (TMDL) Environmental Regulations: Proceedings of the March 11-13, 2002 Conference, pp. 367–376.

Buckerfield, S.J., Quilliam, R.S., Waldron, S., Naylor, L.A., Li, S., Oliver, D.M., 2019. Rainfall-driven E.coli transfer to the stream-conduit network observed through increasing spatial scales in mixed land-use paddy farming karst terrain. Water

Research X 5 (100038). https://doi.org/10.1016/j.wroa.2019.100038. ISSN 2589-9147.
Burnet, J.-B., Habash, M., Hachad, M., Khanafer, Z., Prévost, M., Servais, P., Sylvestre, E., Dorner, S., 2021. Automated targeted sampling of waterborne pathogens and microbial source tracking markers using near-real time monitoring of microbiological water quality. Water (Basel) 13 (15), 2069. https://doi.org/10.3390/w13152069.
Camacho Suarez, V.V., Schellart, A.N.A., Brevis, W., Shucksmith, J.D, 2019a. Quantifying the impact of uncertainty within the longitudinal dispersion coefficient on concentration dynamics and regulatory compliance in rivers. Water Resour. Res. 55, 4393–4409. https://doi.org/10.1029/2018WR023417.
Camacho Suarez, V.V., Brederveld, R.J., Fennema, M., Moreno-Rodenas, A., Langeveld, J., Korving, H., Schellart, A.N.A., Shucksmith, J.D., 2019b. Evaluation of a coupled hydrodynamic-closed ecological cycle approach for modelling dissolved oxygen in surface waters. Environ. Modell. Softw. 119, 242–257.
CEH (2023) 'UKCEH Land Cover® plus: crops', https://www.ceh.ac.uk/data/ceh-land-cover-plus-crops-2015#specs (Accessed 14.05.2023).
Collins, R., Rutherford, K., 2004. Modelling bacterial water quality in streams draining pastoral land. Water Res. 38 (3), 700–712.
DEFRA (2022) 'Structure of the agricultural industry in England and the UK at June – county', Statistical data set, https://assets.publishing.service.gov.uk/government/uploads/system/uploads/attachment_data/file/1084972/structure-england-june21-county-23jun22.ods (Accessed 11.04.2023).
Demeter, K., Burnet, J.-B., Stadler, P., Kirschner, A., Zessner, M., Farnleitner, A.H., 2020. Automated online monitoring of fecal pollution in water by enzymatic methods. Current Opin. Environ. Sci. Health 16, 82–91. https://doi.org/10.1016/j.coesh.2020.03.002. ISSN 2468-5844.
Derx, J., Kılıç, H.S., Linke, R., Cervero-Aragó, S., Frick, C., Schijven, J., Kirschner, A.K.T., Lindner, G., Walochnik, J., Stalder, G., Sommer, R., Saracevic, E., Zessner, M., Blaschke, A.P., Farnleitner, A.H., 2023. Probabilistic fecal pollution source profiling and microbial source tracking for an urban river catchment. Sci. Total Environ. 857 (2), 159533 https://doi.org/10.1016/j.scitotenv.2022.159533. ISSN 0048-9697.
Dienus, O., Sokolova, E., Nystrom, F., Matussek, A., Lofgren, S., Blom, L., Pettersson, T.J. R., Lindgren, P.-E., 2016. Norovirus dynamics in wastewater discharges and in the recipient drinking water source: long-term monitoring and hydrodynamic modeling. Environ. Sci. Technol. 50, 10851–10858.
Dorner, S.M., Anderson, W.B., Slawson, R.M., Kouwen, N., Huck, P.M., 2006. Hydrologic modeling of pathogen fate and transport. Environ. Sci. Technol. 40 (15), 4746–4753.
Du, J., Xie, H., Hu, Y., Xu, Y., Xu, C.-Y., 2009. Development and testing of a new storm runoff routing approach based on time variant spatially distributed travel time method. J. Hydrol. 369 (1–2), 44–54.
DWI (2020) 'Guidance on implementing the water supply (water quality) regulations 2016 (as amended) in England and the water supply (water quality) regulations in (wales) 2018′, part 4 monitoring of water supplies, http://www.dwi.gov.uk/stakeholders/±-guidanceand-codes-of-practice/wswq/index.html (Accessed 15.06.2020).
Ellis, J.B., Yu, W., 1995. Bacteriology of urban runoff: the combined sewer as a bacterial reactor and generator. Wat. Sci. Tech. 31 (7), 303–310.
Environment Act (2021) https://www.legislation.gov.uk/ukpga/2021/30/contents/enacted (Accessed 15.06.2020).
Environment Agency (2023) 'Event duration monitoring - storm overflows - annual returns', https://www.data.gov.uk/dataset/19f6064d-7356-466f-844e-d20ea10ae9fd/event-duration-monitoring-storm-overflows-annual-returns.
EU (2006) 'Directive 2006/7/EC of the European Parliament and of the Council of 15 February 2006 concerning the management of bathing water quality and repealing Directive 76/160/EEC', https://eur-lex.europa.eu/legal-content/EN/TXT/?uri=CELEX:32006L0007 (Accessed 14.05.2023).
Fachs, S., Sitzenfrei, R., Rauch, W., 2008. Assessing the relationship between water level and combined sewer overflow with computational fluid dynamics. Water Sci. Technol. 60 (12), 3035–3043.
Ferguson, C.M., Croke, B.F.W., Beatson, P.J., Ashbolt, N.J., Deere, D.A., 2007. Development of a process-based model to predict pathogen budgets for the Sydney drinking water catchment. J. Water Health 5 (2), 187–208.
Gao, G.H., Falconer, R.A., Lin, B.L., 2015. Modelling the fate and transport of faecal bacteria in estuarine and coastal waters. Mar. Pollut. Bull. 100, 162–168.
García-García, L.M., Campos, C.J.A., Kershaw, S., Younger, A., Bacon, J., 2021. Scenarios of intermittent *E. coli* contamination from sewer overflows to shellfish growing waters: the Dart Estuary case study. Mar. Pollut. Bull. 167, 1–17.
Ghimire, B., Deng, Z., 2013. Hydrograph-based approach to modeling bacterial fate and transport in rivers. Water Res. 47 (3), 1329–1343.
Graydon, R.C., Mezzacapo, M., Boehme, J., Foldy, S., Edge, T.A., Brubacher, J., Chan, H. M., Dellinger, M., Faustman, E.M., Rose, J.B., Takaro, T.K., 2022. Associations between extreme precipitation, drinking water, and protozoan acute gastrointestinal illnesses in four North American Great Lakes cities (2009–2014). J. Water Health 20 (5), 849–862. https://doi.org/10.2166/wh.2022.018.
Guymer, I., 2002. A National Database of Travel Time, Dispersion and Methodologies for the Protection of River Abstractions. Environment Agency, Bristol. ISBN: 1857058216.
Harmel, R.D., Hathaway, J.M., Wagner, K.L., Wolfe, J.E., Karthikeyan, R., Francesconi, W., McCarthy, D.T., 2016. Uncertainty in monitoring *E. coli* concentrations in streams and stormwater runoff. J. Hydrol. 534, 524–533. https://doi.org/10.1016/j.jhydrol.2016.01.040.
Haydon, S., Deletic, A., 2006. Development of a coupled pathogen-hydrologic catchment model. J. Hydrol. 328 (3–4), 467–480.
Hellweger, F.L., Masopust, P, 2008. Investigating the fate and transport Ofescherichia coli in the Charles river, Boston, using high-resolution observation and modeling. J. Am. Water Resour. Assoc. 44 (2), 509–522.
Hubbart, J.A., Kellner, E., Petersen, F.A., 2022. 22-site comparison of land-use practices, e-coli and enterococci concentrations. Int. J. Environ. Res. Public Health 19 (21), 13907. https://doi.org/10.3390/ijerph192113907.
Jalliffier-Verne, I., Leconte, R., Huaringa-Alvarez, U., Heniche, M., Madoux-Humery, A.-S., Autixier, L., Galarneau, M., Servais, P., Prévost, M., Dorner, S., 2017. Modelling the impacts of global change on concentrations of Escherichia coli in an urban river. Adv. Water Resour. 108, 450–460.
Jiang, G., Guo, F., Wei, L., Li, W., 2023. Characterizing the transitory groundwater-surface water interaction and its environmental consequence of a riverside karst pool. Sci. Total Environ. 902, 166532 https://doi.org/10.1016/j.scitotenv.2023.166532. ISSN 0048-9697.
Joseph, N., Lucas, J., Viswanath, N., Findlay, R., Sprinkle, J., Strickland, M.S., Winford, E., Kolok, A.S., 2021. Investigation of relationships between fecal contamination, cattle grazing, human recreation, and microbial source tracking markers in a mixed-land-use rangeland watershed. Water Res. 194, 116921 https://doi.org/10.1016/j.watres.2021.116921. ISSN 0043-1354.
Jovanovic, D., Hathaway, J., Coleman, R., Deletic, A., McCarthy, D., 2017. Conceptual modelling of *E. coli* in urban stormwater drains, creeks and rivers. J. Hydrol. (Amst) 555, 129–140.
Kammouna, R., McQuaida, N., Lessardb, V., Prévost, M., Bichai, F., Dorner, S., 2023. Comparative study of deterministic and probabilistic assessments of microbial risk associated with combined sewer overflows upstream of drinking water intakes. Environ. Challenges 12 (100735).
Leonhardt, G., D'Oria, M., Kleidorfer, M., Rauch, W., 2014. Estimating inflow to a combined sewer overflow structure with storage tank in real time: evaluation of different approaches. Water Sci. Technol. 70 (7), 1143–1151. https://doi.org/10.2166/wst.2014.331.
Madoux-Humery, A., Dorner, S., Sebastien, S., Aboulfadl, K., Galarneau, M., Servais, P., Prévost, M, 2013. Temporal variability of combined sewer overflow contaminants: evaluation of wastewater micropollutants as tracers of fecal contamination. Water Res. 47, 4370–4382.
Madoux-Humery, A.S., Dorner, S.M., Sauve, S., Aboulfadl, K., Galarneau, M., Servais, P., Prevost, M., 2015. Temporal analysis of *E. coli*, TSS and wastewater micropollutant loads from combined sewer overflows: implications for management. Environ. Sci. Process. Impacts 17 (5), 965–974.
Madoux-Humery, A.-S., Dorner, S., Sebastien, S., Aboulfadl, K., Galarneau, M., Servais, P., Prévost, M., 2016. The effects of combined sewer overflow events on riverine sources of drinking water. Water Res. 92, 218–227.
Mancini, M., Rosso, R., 1989. Using GIS to assess spatial variability of SCS Curve Number at the basin scale. In New directions for surface water modelling. In: Proceedines of the Baltimore Symposium. IAHS, pp. 435–444, 181.
Marsalek, J., Rochfort, Q., 2004. Urban wet-weather flows: sources of fecal contamination impacting on recreational waters and threatening drinking-water sources. J. Toxicol. Environ. Health Part A 67 (20–22), 1765–1777.
McGechan, M.B., Vinten, A.J.A., 2003. Simulation of transport through soil of *E. coli* derived from livestock slurry using the MACRO model. Soil Use Manag. 19, 321–330.
McKergow, L.A., Davies-Colley, R.J., 2010. Stormflow dynamics and loads of Escherichia coli in a large mixed land use catchment. Hydrol. Process 24 (3), 276–289.
Melesse, A.M., Graham, W.D., 2004. Storm runoff prediction based on a spatially distributed travel time method utilizing remote sensing and GIS. J. Am. Water Resour. Assoc. 40 (4), 863–879.
Moreno-Rodenas, A.M., Tscheikner-Gratl, F., Langeveld, J.G., Clemens, F.H.L.R., 2019. Uncertainty analysis in a large-scale water quality integrated catchment modelling study. Water Res. 158, 46–60. https://doi.org/10.1016/j.watres.2019.04.016. ISSN 0043-1354.
Neill, A.J., Tetzlaff, D., Strachan, N.J.C., Hough, R.L., Avery, L.M., Maneta, M.P., Soulsby, C., 2020. An agent-based model that simulates the spatio-temporal dynamics of sources and transfer mechanisms contributing faecal indicator organisms to streams. Part 2: application to a small agricultural catchment. J. Environ. Manage. 270 https://doi.org/10.1016/j.jenvman.2020.110905, 110905, ISSN 0301-4797.
NRFA (2023) '54050 - Leam at Eathorpe', https://nrfa.ceh.ac.uk/data/station/info/54050 (Accessed 28.10.2023).
Oliver, D.M., Fish, R.D., Hodgson, C.J., Heathwaite, A.L., Chadwick, D.R., Winter, M., 2009. A cross-disciplinary toolkit to assess the risk of faecal indicator loss from grassland farm systems to surface waters. Agricult., Ecosyst. Environ. 129, 401–412.
Oliver, D.M., Porter, K.D., Heathwaite, A.L., Zhang, T., Quilliam, R.S., 2015. Impact of low intensity summer rainfall on *E. coli*-discharge event dynamics with reference to sample acquisition and storage. Environ. Monit. Assess. 187 (7), 426. https://doi.org/10.1007/s10661-015-4628-x.
Oliver, D.M., Bartie, P.J., Heathwaite, A.L., Reaney, S.M., Parnell, J.A.Q., Quilliam, R.S., 2018. A catchment-scale model to predict spatial and temporal burden of *E. coli* on pasture from grazing livestock. Sci. Total Environ. 616-617, 678–687.
Ordnance Survey (2023) 'Built Up Areas (2022)', Dataset, https://osdatahub.os.uk/downloads/open/BuiltUpAreas.
Owolabi, T.A., Mohandes, S.R., Zayed, T., 2022. Investigating the impact of sewer overflow on the environment: a comprehensive literature review paper. J. Environ. Manage. 301, 113810 https://doi.org/10.1016/j.jenvman.2021.113810. ISSN 0301-4797.
Rutherford, J.C., (1994) John Wiley & Sons, Chichester, ISBN 0-471-94282-0.
Sadeghi, A.M., Arnold, J.G., 2002. A SWAT/microbial sub-model for predicting pathogen loadings in surface and groundwater at watershed and basin scales. In: Total Maximum Daily Load (TMDL) Environmental Regulations: Proceedings of the March 11-13, 2002 Conference, (Fort Worth, Texas, USA) 701P0102, pp. 56–63.

Sartory, D.P., Howard, L., 1992. A medium detecting beta-glucuronidase for the simultaneous membrane filtration enumeration of Escherichia coli and coliforms from drinking water. Lett. Appl. Microbiol. 15, 273–276.
Schijven, J., Derx, J., de Roda Husman, A.M., Blaschke, A.P., Farnleitner, A.H., 2015. QMRAcatch: microbial quality simulation of water resources including infection risk assessment. J. Environ. Qual. 44 (5), 1491–1502.
Seis, W., Zamzow, M., Caradot, N., Rouault, P., 2018. On the implementation of reliable early warning systems at European bathing waters using multivariate Bayesian regression modelling. Water Res. 143, 301–312.
Shepherd, W., Mounce, S., Sailor, G., Gaffney, J., Shah, N., Smith, N., Cartwright, A., Boxall, J., 2023. Cloud-based artificial intelligence analytics to assess combined sewer overflow performance. J. Water Resour. Plann. Manage. 149 (10) https://doi.org/10.1061/JWRMD5.WRENG-5859.
Sokolova, E., Pettersson, T.J.R., Bergstedt, O., Hermansson, M., 2013. Hydrodynamic modelling of the microbial water quality in a drinking water source as input for risk reduction management. J. Hydrol. 497, 15–23.
Srivastava, A.K., Tait, S., Schellart, A., Kroll, S., Van Dorpe, M., Van Assel, J., Shucksmith, J., 2018. Quantifying Uncertainty in Simulation of Sewer Overflow Volume. ASCE J. Environ. Eng. 144 (7), 1–10.
Sterk, A., Schijven, J., de Roda Husman, A.M., de Nijs, T., 2016. Effect of climate change on runoff of Campylobacter and Cryptosporidium from land to surface water. Water Res. 95, 90–102.
Suslovaite, V., 2023. Development of a risk based approach to surface water abstraction. PhD thesis, University of Sheffield.
Taghipour, M., Shakibaeinia, A., Sylvestre, E., Tolouei, S., Dorner, S., 2019. Microbial risk associated with CSOs upstream of drinking water sources in a transboundary river using hydrodynamic and water quality modeling. Sci. Total Environ. 683, 547–558.
The standing Committee of Analysts (2016) 'The Microbiology of Drinking Water (2016) - Part 4 Methods for the isolation and enumeration of coliform bacteria and Escherichia coli (including *E. coli* O157:h7)'.
Tscheikner-Gratl, F., Bellos, V., Schellart, A., Moreno-Rodenas, A., Muthusamy, M., Langeveld, J., Clemens, F., Benedetti, L., Angel Rico-Ramirez, M., Fernandes de Carvalho, R., Breuer, L., Shucksmith, J., Heuvelink, G.B.M., Tait, T., 2019. Recent insights on uncertainties present in integrated catchment water quality modelling. Water Res. 150, 368–379.
UKCEH (2023) 'Flood Estimation Handbook Web Service', https://fehweb.ceh.ac.uk/Map (Accessed 14.05.2023).
USEPA, 2008. In: Results of the Interlaboratory Testing Study for the Comparison of Methods for Detection and Enumeration of Enterococci and Escherichia coli in Combined Sewer Overflows (CSOs). Environmental Protection Agency, Office of Water, Washington, DC. EPA-821-R-08-006.
Vesuviano, G., 2022. The FEH22 rainfall depth duration-frequency (DDF) model. UK Centre Ecol. Hydrol. 1–102.
Wallis, S.G., Young, P.C., Beven, K.J., 1989. Experimental investigation of the aggregated dead zone model for longitudinal solute transport in stream channels. Proc. Instn Ciu. Engrs. 87, 1–22.
Walker, F.R., Stedinger, J.R., 1999. Fate and transport model of cryptosporidium. J. Environ. Eng. 125 (4), 325–333.
Whelan, G., Kim, K., Pelton, M.A., Soller, J.A., Castleton, K.J., Molina, M., Pachepsky, Y., Zepp, R., 2014. An integrated environmental modeling framework for performing quantitative microbial risk assessments. Environ. Model. Softw. 55, 77–91.
Wiesner-Friedman, C., Beattie, R.E., Stewart, J.R., Hristova, K.R., Serre, M.L., 2022. Characterizing differences in sources of and contributions to fecal contamination of sediment and surface water with the microbial FIT framework. Environ. Sci. Technol. 56 (7), 4231–4240. https://doi.org/10.1021/acs.est.2c00224.
Wong, T.S.W., 2003. Comparison of celerity-based with velocity-based time-of-concentration of overland plane and time-of-travel in channel with upstream inflow. Adv. Water Resour. 26 (11), 1171–1175.
Yassin, M., Asfaw, A., Speight, V., Shucksmith, J.D., 2021. Evaluation of data-driven and process-based real-time flow forecasting techniques for informing operation of surface water abstraction. J. Water Resour. Plann. Manage. 147 (7), 1–14.
Young, P.C., Wallis, S.G., 1986. The aggregated dead zone (ADZ) model for dispersion in rivers. In: Int. Conf. on Wat. Qual. Modelling in the Inland Nat. Env., Bournemouth, Eng., L1, pp. 421–433.
Zan, R., Blackburn, A., Plaimart, J., Acharya, K., Walsh, C., Stirling, R., Kilsby, C.G., Werner, D., 2023. Environmental DNA clarifies impacts of combined sewer overflows on the bacteriology of an urban river and resulting risks to public health. Sci. Total Environ. 889 (164282) https://doi.org/10.1016/j.scitotenv.2023.164282. ISSN 0048-9697.